



Direct detection of HO₂ radicals in the vicinity of TiO₂ photocatalytic surfaces using cw-CRDS

Chiheb Bahrini, Alexander Parker, Coralie Schoemaecker, Christa Fittschen*

PhysicoChimie des Processus de Combustion et de l'Atmosphère PC2A, University Lille 1, Cité Scientifique, Bât. C11, 59655 Villeneuve d'Ascq, France

ARTICLE INFO

Article history:

Available online 30 July 2010

Keywords:

Photocatalysis
Remote oxidation
HO₂ radicals

ABSTRACT

This work describes the first ever direct detection of HO₂ radicals in the gas phase above photocatalytic surfaces. A glass plate covered with TiO₂ has been illuminated in the presence of H₂O₂ by a 20 W fluorescence lamp centred at 365 nm. The activity of the photocatalytic material has been proven through direct, time resolved observation of the degradation of H₂O₂ by following its concentration by the very sensitive and selective technique of cw-Cavity Ring Down Spectroscopy (cw-CRDS). An absorption line of H₂O₂ at 6639.89 cm⁻¹ has been used, permitting a detection limit of [H₂O₂]_{min} = 1.3 and 3.6 × 10¹³ cm⁻³ for 50 and 200 Torr of synthetic air, respectively. A lower limit of the quantum yield for H₂O₂ degradation has been estimated to $\phi_{min} = 0.0024$. Under the same conditions, the formation of HO₂ radicals has been detected directly and selectively in the gas phase, using the same technique. HO₂ radicals have been observed at up to 4 cm above the surface and at total pressures of up to 230 Torr.

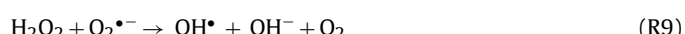
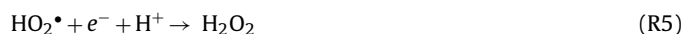
© 2010 Elsevier B.V. All rights reserved.

1. Introduction

Photocatalysis has found many applications since it was first described in 1972 by Fujishima and Honda [1]. Water and air purification can be considered as a major challenge of the years to come and photocatalysis can play a major role in these fields [2]. However, the detailed mechanism is still not well understood and new experimental approaches can help to obtain a more complete picture. This paper describes the application of continuous wave-Cavity Ring Down Spectroscopy (cw-CRDS), a sensitive absorption technique readily used in spectroscopy, but so far only rarely applied to the study of photocatalytic processes [3,4]. This technique permits the direct, *in situ* and time resolved investigation of the composition of the gas phase in the vicinity of a photocatalytic surface.

Photocatalytic processes use a semi-conductor photocatalyst, usually TiO₂, as slurry or deposited on a support. The semi-conductor, exposed to near UV-light ($\lambda < 387$ nm), is able to generate electron-hole pairs (e^-/h^+). Those excitons can migrate into the semi-conductor lattice and reach the surface. They are subsequently available for oxydo-reduction reactions. Heterogeneous reactions with the gas phase components (O₂, H₂O, hydrocarbons) lead to the formation of Reactive Oxygenated Species (ROS) such as OH[•], HO₂[•], H₂O₂ [5,6] and O₂(¹Δ) [7–9]. The main reactions can

be described as following:



Based on the above mechanism, it is believed that the ROS are formed on the surface of the catalyst, and that the photocatalytic degradation occurs when these adsorbed ROS species react with adsorbed organic compounds [10].

However, several authors have found indirect evidence of the diffusion of ROS into the gas phase.

Lee and Choi [11] have studied the photocatalytic oxidation of soot film deposited on a substrate partially covered with TiO₂ and have observed the degradation of soot particles being deposited without direct contact with the TiO₂ surface: from this observation they have first highlighted the possible diffusion of OH[•] radicals into the gas phase during the photocatalytic degradation. A similar

* Corresponding author. Tel.: +33 3 20 33 72 66; fax: +33 3 20 43 69 77.

E-mail address: christa.fittschen@univ-lille1.fr (C. Fittschen).

experiment by Park and Choi [12] using stearic acid led to the same conclusion. Furthermore, they have shown that the remote photocatalytic oxidation is mediated by active oxygen species diffusing through organic polymer membrane over surface-fluorinated TiO_2 [13]. To conclude, Choi and co-workers have observed the migration of OH^\bullet radicals in all media (gas, liquid and solid phases) during a photocatalytic process.

Tatsuma et al. [14,15] have used other indirect methods in order to evidence the diffusion of ROS into the gas phase. They observed the degradation of different organic films separated by an air gap (50 μm to 2.2 mm) from the TiO_2 photocatalytic material. Investigations with the colorimetric method performed by Kubo et al. [16,17] on hydrogen peroxide formation by the exposure of TiO_2 to UV radiation demonstrated the presence of H_2O_2 in gas flowing out of the photocatalyst.

The first successful direct detection of the presence of OH^\bullet radicals near the surface of TiO_2 was reported by Murakami et al. [18,19] using LIF spectroscopy at very low pressure (0.5 Torr). They studied several parameters such as the distance from the surface (5–8 mm), the gas nature (He, H_2O , D_2O and O_2) and the influence of calcinations temperature on the OH-LIF intensity. Following this work, Vincent et al. [20] and Thiebaud et al. [21] have also reported the use of LIF technique in connection with laser photolysis for detection of OH^\bullet radicals close to the TiO_2 surface in the gas phase. They observed both OH and H_2O_2 even at elevated pressures and at distances of several mm from the surface. However, a drawback of these direct detections is the high photon flux used in these experiments (several orders of magnitude higher than usual photocatalytic conditions), due to the use of pulsed lasers.

However, HO_2^\bullet radicals have not yet been detected in photocatalytic processes. A recent attempt by our group to detect these radicals during the photocatalytic degradation of methyl ethyl ketone by cw-CRDS [3] was not successful, with no radicals being observed while the estimated detectable concentration was $3 \times 10^9 \text{ cm}^{-3}$. In the former work we adapted a reactor that had been originally designed for gas phase spectroscopic studies. Therefore, one of the reasons for the absence of detectable HO_2^\bullet radicals was that the cw-CRDS absorption path was not well positioned with respect to the TiO_2 surface and the irradiation source. Recently, we have designed and constructed a new reactor, optimized for analyzing the gas phase composition in the vicinity of a surface by cw-CRDS. In this paper, we present the details of the reactor as well as the first results obtained using this experimental set-up.

2. Experimental

A new reactor has been constructed, dedicated to the in situ analysis of the gas phase above photocatalytic surfaces, using cw-CRDS. The schematic view of the set-up is shown in Fig. 1: the reactor consists of a rectangular cell made of aluminium with inner dimensions of $68 \text{ cm} \times 8.5 \text{ cm} \times 4 \text{ cm}$, i.e. a total volume of 2300 cm^3 . Photocatalytic surfaces with a dimension of up to $65 \text{ cm} \times 3.5 \text{ cm}$ can be positioned horizontally thanks to two vertical motion feedthroughs. This way, the photocatalytic surface is fixed parallel to the optical pathway, which itself is positioned 2 cm above the upper rim of the cell or 6.5 cm from the bottom of the reactor: taking into account the mounting, the maximum distance between photocatalytic surface and detection volume can be varied by up to 5 cm. The upper side of the cell is closed by 2 quartz windows ($35 \text{ cm} \times 4.5 \text{ cm}$) with a free aperture of $33 \text{ cm} \times 3.4 \text{ cm}$, permitting the irradiation of a surface of up to 66 cm long. However, in these experiments the fluorescence lamp (UVP, 50 cm long, centred at 365 nm) limited the irradiated surface. The lamp can be fixed at variable distances above the cell: the minimum distance between the centre of the lamp and the surface is 7 cm,

leading to a maximum irradiation power of 9 mW cm^{-2} , equal to $1.6 \times 10^{16} \text{ photons cm}^{-2} \text{ s}^{-1}$. Positioning the surface at the lowest possible position leads to a distance between lamp and surface of 12 cm and hence an irradiation power of 5.3 mW cm^{-2} , equal to $9.5 \times 10^{15} \text{ photons cm}^{-2} \text{ s}^{-1}$.

The HO_2 detection in the gas phase is based on our previous work [22]: we have shown that a sensitive and selective detection of HO_2 radicals can be achieved by cw-CRDS in the near infrared range. More recently, we have published the absorption spectrum of HO_2 between 6604 and 6696 cm^{-1} including the absolute absorption cross-sections of the most intense lines in this range [23]. The strongest line was observed at 6638.20 cm^{-1} and it exhibits a cross-section of $\sigma_{6638.20 \text{ cm}^{-1}} = 2.72 \times 10^{-19} \text{ cm}^2$ at 50 Torr Helium. The present work was therefore carried out at this wavenumber – at the centre of the strongest line – in order to obtain as low a detection limit as possible. The pressure broadening coefficients of several absorption lines have been measured [24] and have been used to calculate the absorption cross-sections for the experimental conditions used in this work. H_2O_2 has also been detected by cw-CRDS. We have quantified its concentration using an absorption line at 6639.89 cm^{-1} . In a very recent work, we have measured the absorption cross-section using a combination of time resolved LIF and cw-CRDS (ref to be published).

The near-infrared beam was provided by a fibred distributed feed-back (DFB) diode laser (Fitel-Furukawa FOL15DCWB-A81-W1509) emitting up to 40 mW in the wavelength range $6640 \pm 13 \text{ cm}^{-1}$. The diode laser emission is directly fibred and passes through a fibred optical isolator and fibred 90/10% beam splitter. The 10% portion is connected to a fibred wavemeter (Burleigh WA-1100) with an accuracy of 0.01 cm^{-1} for monitoring the wavelength of the laser emission. The remaining 90% is coupled into the CRDS optical cavity through a short focal length lens ($f = 12 \text{ mm}$) for mode matching so as to excite the fundamental TEM_{00} mode. Two folding mirrors allow easy alignment of the beam, while an acousto-optical modulator (AOM, Gooch and Housego), is positioned between the mirrors as shown in Fig. 1. The AOM allows the laser beam to be deviated within 350 ns with respect to a trigger signal for a total of 440 μs . The optical signal transmitted through the cavity is converted into current by an avalanche photodiode (Perkin Elmer C30662E). An in-house designed amplifier-threshold circuit converts the current signal to an exploitable voltage signal and triggers the AOM to deviate the laser beam as soon as the cavity comes into resonance and the photodiode signal passes a user-defined threshold. The photodiode signal is connected to a fast 16 bit analogue acquisition card (PCI-6259, National Instruments) in a PC, which is triggered also by the amplifier-threshold circuit. The acquisition card has an acquisition frequency of 1.25 MHz and thus the ring-down signal is sampled every 800 ns and the data are transferred to PC in real time via PCI bus. This approach allows clean and reproducible exponential decays to be obtained. The ring-down time τ is obtained by fitting the exponential decay over a time range of seven lifetimes by a Levenberg–Marquardt exponential fit in LabView. The concentration of a species being formed in the gas phase or consumed in the photocatalytic process, can be obtained by measuring the ring-down time of the empty cavity τ_0 , i.e. the ring down time before turning on the UV-lamps, and the ring down time τ , after turning on the UV-lamps:

$$\alpha = [A] \times \sigma = \frac{R_L}{c} \left(\frac{1}{\tau} - \frac{1}{\tau_0} \right) \quad (1)$$

where σ is the absorption cross-section, R_L is the ratio between the cavity length L , i.e. the distance between the two cavity mirrors to the length L_A over which the absorber is present (in the case of short-lived radical species the length of the photocatalytic surface, in the case of long-lived species the distance of the cavity mirrors),

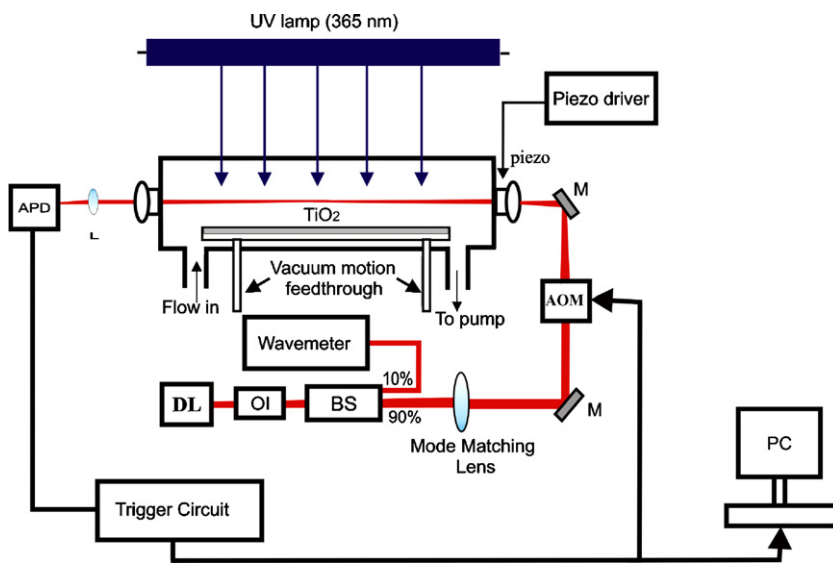


Fig. 1. Schematic view of the experimental set-up.

c is the speed of light. Knowing the absorption cross-section σ , one can extract the concentration $[A]$ of the target molecule.

The present work was carried out at pressures between 30 and 233 Torr synthetic air. HO_2 radicals were detected at a wavenumber of 6638.20 cm^{-1} and from the known broadening coefficients of the HO_2 absorption lines [24], we obtain absorption cross-sections varying from 1.98 to $0.67 \times 10^{-19} \text{ cm}^2$ for 50 and 200 Torr synthetic air, respectively. Under these conditions, we estimate a minimum detectable concentration of $[\text{HO}_2]_{\min} = 7$ and $20 \times 10^9 \text{ cm}^{-3}$ for 50 and 200 Torr synthetic air, respectively, after averaging ring-down signals over 1 s. H_2O_2 was detected at a wavenumber of 6639.89 cm^{-1} , where the absorption cross-section at 50 Torr Helium has recently been determined [25] to be $\sigma = 1.35 \times 10^{-22} \text{ cm}^2$. However, the broadening coefficients are not known, so we have assumed the same broadening coefficients as for HO_2 [24]. Doing so, we obtain absorption cross-sections for H_2O_2 of 9.86×10^{-23} and $3.34 \times 10^{-23} \text{ cm}^2$ at 50 and 200 Torr synthetic air, respectively. Under these conditions, we estimate a minimum detectable concentration of $[\text{H}_2\text{O}_2]_{\min} = 1.3$ and $3.6 \times 10^{13} \text{ cm}^{-3}$ for 50 and 200 Torr synthetic air, respectively, after averaging ring-down signals over 1 s.

The cell is operated in a quasi-static way, small gas flows through the cell are admitted through calibrated flow meters. Various flows (between 1 and 20 STP $\text{cm}^3 \text{ min}^{-1}$) of pure O_2 were bubbled through a solution of 50% H_2O_2 in water. These flows were diluted with various flows (between 20 and 80 STP $\text{cm}^3 \text{ min}^{-1}$) of synthetic air before entering the cell. The total volume of the cell being 2300 cm^3 , this leads to a typical residence time of 200–300 s.

3. Results

3.1. Evidence of photocatalytic activity

The activity of the photocatalytic surface and the performance of the experimental set-up have first been tested by measuring the decrease of H_2O_2 concentration in the gas phase due to the photocatalytic process. Fig. 2 shows the H_2O_2 absorption spectrum around 6639.9 cm^{-1} obtained after admitting a total flow of 50 STP $\text{cm}^3 \text{ min}^{-1}$, 1 STP $\text{cm}^3 \text{ min}^{-1}$ of which was bubbled through H_2O_2 at a total pressure of 34 Torr. The ring-down time of the empty cell, i.e. before admitting H_2O_2 to the main flow, is governed by the reflectivity of the mirrors, as shown in Eq. (1), and was $38.95 \mu\text{s}$, indicated as a dashed line. The absorption line at 6639.89 cm^{-1} has

been calibrated in an earlier work [25] and allows to calculate the absolute H_2O_2 concentration to be $2.6 \times 10^{14} \text{ cm}^{-3}$. Fig. 3a shows the evolution of the ring-down time at 6639.89 cm^{-1} under the same conditions, when turning on and off the UV-lamps. These ring-down times have been converted to total H_2O_2 concentration by applying Eq. (1) and are shown in Fig. 3b. The initial H_2O_2 concentration in the reaction cell of $2.6 \times 10^{14} \text{ cm}^{-3}$ slowly decreases after turning on the lamps, before reaching a steady state concentration of $1.4 \times 10^{14} \text{ cm}^{-3}$ after around 140 s. The total flow in this experiment was $50 \text{ STP cm}^{-3} \text{ min}^{-1}$ at a total pressure of 34 Torr, leading to a residence time of 120 s, in good agreement with the decay times when turning on the UV-lamp. Turning off the UV-lamps results in the ring-down time slowly returning to the initial value of $2.6 \times 10^{14} \text{ cm}^{-3}$. However, it seems that after a rapid increase to a H_2O_2 concentration of around $2.0 \times 10^{14} \text{ cm}^{-3}$ during the first 100 s, a second much slower increase follows over several 100 s. Repeating the experiment always led to this observation, so we tentatively explain this by a prolonged activity of the TiO_2 substrate.

From Fig. 3b we can calculate that a total of $1.2 \times 10^{14} \text{ cm}^{-3}$ of H_2O_2 are consumed in the photocatalytic process. From these values, we can estimate a quantum yield for the H_2O_2 -photodegradation: a total of 2.8×10^{17} molecules of H_2O_2 are consumed in the reactor during the photocatalytic activity, assum-

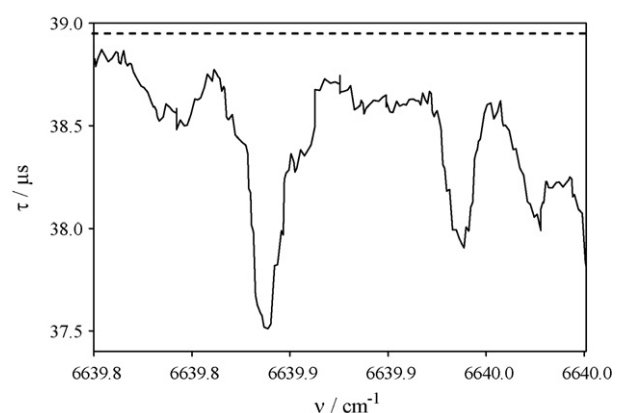


Fig. 2. Absorption spectrum of H_2O_2 , obtained without irradiation at $p = 34$ Torr with $1 \text{ STP cm}^3 \text{ min}^{-1} \text{ O}_2$ through a 50% H_2O_2 mixture, total flow $50 \text{ STP cm}^3 \text{ min}^{-1}$, distance between TiO_2 -support and cw-CRDS absorption path: 48 mm. Baseline τ_0 is indicated as dashed line.

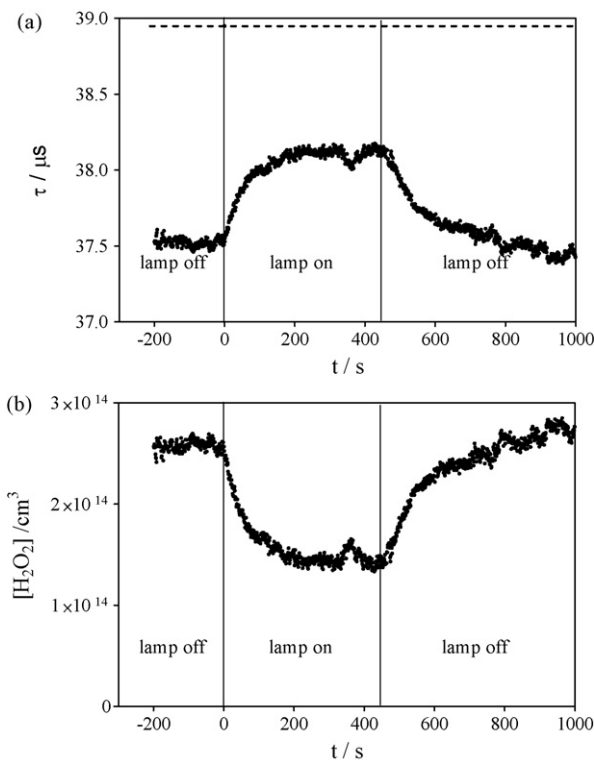


Fig. 3. (a) Evolution of the ring-down time at 6639.98 cm^{-1} as a function of time, UV lamp was turned on at $t=0\text{ s}$ and turned off at $t=440\text{ s}$, experimental conditions are the same as in **Fig. 2**, the distance between TiO_2 -support and cw-CRDS absorption path: 48 mm. (b) Ring-down times have been transformed into concentrations using a baseline of $38.95\text{ }\mu\text{s}$ (obtained in **Fig. 2** and indicated as dashed line) and $\sigma=1.22\times 10^{-22}\text{ cm}^{-2}$.

ing a homogeneous mixture in the entire volume. Divided by the residence time this leads to an H_2O_2 consumption of $2.3\times 10^{15}\text{ s}^{-1}$. The surface was in the lowest possible position ($9.5\times 10^{15}\text{ photons cm}^{-2}\text{ s}^{-1}$) and around 100 cm^2 of photocatalytic surface are irradiated: with these assumptions we calculate a quantum yield of 0.0024 for the H_2O_2 degradation. However, given the observation that the H_2O_2 concentration decreases to low concentrations, this value could be a lower limit if the degradation process is limited rather by the supply of fresh H_2O_2 than by the photocatalytic process itself. On the other hand, the OH radical, a possible primary degradation product, can destroy another H_2O_2 molecule, and therefore increase the H_2O_2 destruction leading to an apparently higher quantum yield. Future experiments are planned using UV-LEDs as light source: the irradiation intensity can easily be varied and more precise quantum yields can be determined.

3.2. Evidence of HO_2 formation

In order to investigate the formation of HO_2 radicals in the gas phase above the photocatalytic surface, we have scanned a portion of the spectrum around the most intense absorption line [23]. In this type of experiment, we typically average over 50 ring-down signals before incrementing the wavelength emitted by the diode by typically 0.0013 cm^{-1} . Measuring the spectrum in the wavenumber range $6637.3\text{--}6638.8\text{ cm}^{-1}$ as shown in **Fig. 4** takes around 20 min. The lower part of the figure, shown as a dotted line, represents the absolute HO_2 absorption spectrum in 50 Torr He and is taken from our earlier work [23]: the line at 6638.21 cm^{-1} is the most intense absorption feature in this wavelength range with an absorption cross-section of $2.72\times 10^{-19}\text{ cm}^2$ at 50 Torr. The upper part of the figure shows the evolution of the ring-down time as a function of

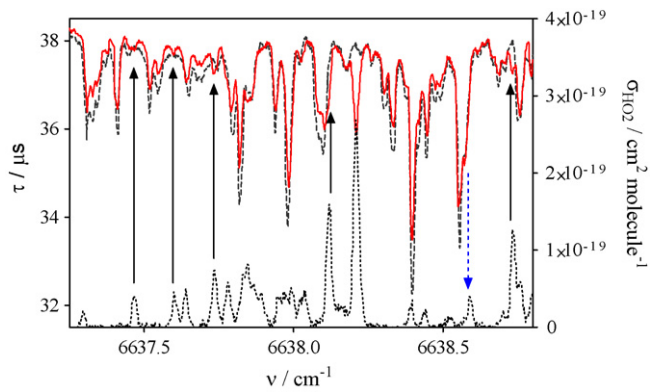


Fig. 4. Ring-down time as a function of wavenumber (left Y-axis), obtained at 183 Torr $\text{O}_2/\text{N}_2/\text{H}_2\text{O}_2$, distance between TiO_2 -support and cw-CRDS absorption path: 4 mm. Red line UV-lamp on, black dashed line UV-lamp off. The HO_2 spectrum (right Y-axis), shown as dotted line, is taken from our earlier work [1].

the wavenumber, now in the presence of H_2O_2 with UV-light off (black, dotted line) and with UV-light on (red, full line). According to Eq. (1), a lower ring-down time corresponds to a higher absorbance, i.e. the opposite of the HO_2 absorption spectrum. The build-up of HO_2 radicals in the gas phase after turning on the UV-light can be observed very clearly and without fail. While the intense line at 6638.21 cm^{-1} is easily visible and not disturbed at all by overlapping H_2O_2 absorption lines, some other absorption features of HO_2 are not so easily visible and have been indicated by arrows. The opposite, i.e. an increase in ring-down time after turning on the UV-light, can be observed at wavelength corresponding to H_2O_2 absorption lines and confirms the observation already demonstrated in **Fig. 3**. The HO_2 -absorption line at 6638.59 cm^{-1} , indicated by the dashed arrow, is not visible in the upper part, in contrast to the comparably intense line at 6637.46 cm^{-1} . This is probably due to compensation by a simultaneous opposite change in ring-down time due to decreased H_2O_2 concentration. To illustrate the sensitivity of our instrument, we have calculated the concentration of HO_2 radicals in the example of **Fig. 4** to be $6.9\times 10^{11}\text{ cm}^{-3}$.

3.3. Influence of gas phase photolysis

It is well known that H_2O_2 absorbs even at wavelengths above 300 nm, probably leading to the formation of OH radicals with a yield of $\Phi=2$ [26]. The absorption spectrum, taken from Atkinson et al. [27], is reproduced in **Fig. 5a** together with the emission spectrum of our UV-lamp, with the convolution of both graphs represented in **Fig. 5b**. One can observe a non-negligible overlap of both absorption and lamp spectrum and hence the possibility of direct H_2O_2 photolysis. OH radicals will rapidly be transformed under our experimental conditions into HO_2 radicals through the following reaction



Therefore, it is indispensable to verify that the observed consumption of H_2O_2 in **Fig. 3** and the observed formation of HO_2 radicals in **Fig. 4** are indeed due to photocatalytic activity and not due to gas phase photolysis of H_2O_2 by UV-light. We have therefore performed blank experiments, i.e. in the absence of any photocatalytic material. In **Fig. 6** three HO_2 concentration time profiles are shown, the lower two traces were recorded at 33 Torr using an H_2O_2 concentration of $2.5\times 10^{14}\text{ cm}^{-3}$: in both cases the UV lamp was turned on at $t=0\text{ s}$ and turned off at $t=220\text{ s}$. The signal represented by the black line was obtained in the presence of the photocatalytic substrate, while the lower trace, shown as a dotted line, was the blank experiment: the formation of HO_2 radicals during blank

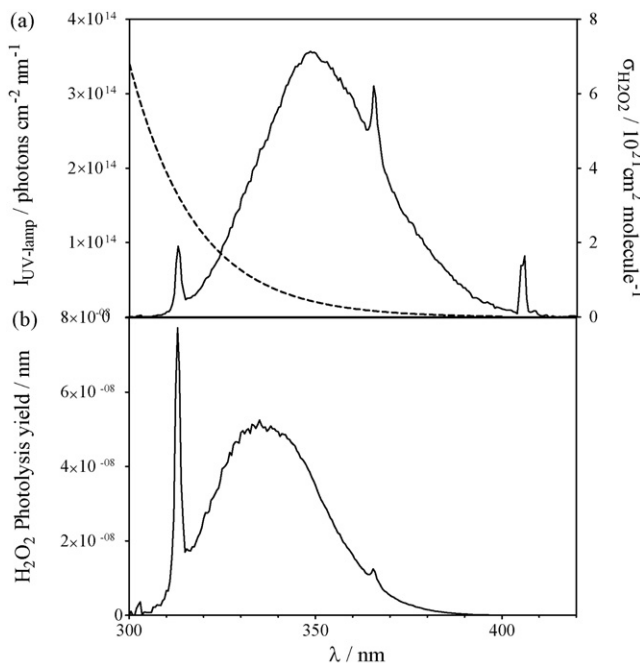


Fig. 5. (a) Dotted line and right y-axis: H₂O₂ absorption spectrum, full line and left y-axis: UV-lamp emission spectrum at 7 cm from the centre of the lamp. (b) Convolution of lamp emission and H₂O₂ absorption spectra.

experiment is clearly below our detection limit under typical reaction conditions and the build-up of HO₂ radicals in the gas phase can therefore clearly be assigned to photocatalytic activity

In order to validate our set-up, we have greatly increased the H₂O₂ concentration to $2.4 \times 10^{15} \text{ cm}^{-3}$, i.e. ten times higher than our typical conditions, in order to make the HO₂ formation from gas phase photolysis visible. The result is shown in Fig. 7 where a small HO₂ build-up is clearly visible. Integrating the data from Fig. 5b we obtain a photolysis rate for H₂O₂ at 7 cm from the UV-lamp of $J = 4 \times 10^{-6} \text{ s}^{-1}$, leading to an OH-production of $1.3 \times 10^{10} \text{ cm}^{-3} \text{ s}^{-1}$ and, according to (R11), an HO₂ production of $2.6 \times 10^{10} \text{ cm}^{-3} \text{ s}^{-1}$. This value needs to be compared with the stationary HO₂ concentration of $2 \times 10^{10} \text{ cm}^{-3}$ measured in Fig. 7. However, this comparison is unfortunately not straight forward because the stationary concentration of HO₂ is strongly influenced by heterogeneous loss of HO₂ radicals. In fact, the self-reaction of

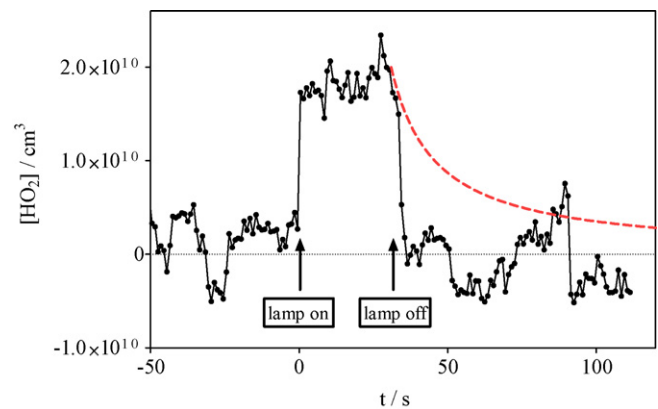


Fig. 7. Blank experiment: formation of HO₂ from the photolysis of H₂O₂ in the absence of photocatalytic surfaces. Dashed red line is the simulated HO₂ decay taking only gas phase reactions into account.

HO₂ in the gas phase



is well known ($k_{11} = 1.7 \times 10^{-12} \text{ cm}^3 \text{ s}^{-1}$, [27]) and rather slow at HO₂-concentrations in the range of 10^{10} or 10^{11} cm^{-3} . Without heterogeneous loss reactions we would therefore expect a slow increase in HO₂ concentration after turning on the UV-lamp until the equilibrium:

Loss through (R12)

$$= \text{Production from photolysis} = 2.6 \times 10^{10} \text{ cm}^{-3} \text{ s}^{-1}$$

is reached. From k_{12} we calculate that this equation is valid at HO₂-concentrations of the order of $1 \times 10^{11} \text{ cm}^{-3}$, hence we would expect an increase in HO₂ concentration lasting several seconds up to a stationary concentration of $1 \times 10^{11} \text{ cm}^{-3}$. However, we observe the stationary state in less than one second at a concentration 5 times lower than estimated. The same observation occurs when turning off the UV-lamp: at an HO₂-concentration of $2 \times 10^{10} \text{ cm}^{-3}$ the decay caused by (R12) is very slow, after 10 s for example a concentration of $1.2 \times 10^{10} \text{ cm}^{-3}$ is reached: the red, dashed curve in Fig. 7 shows the HO₂ decay simulated with only (R12) taken into account. Even though the signal-to-noise ratio is not very good, it is clear, that the HO₂ concentration in our cell decays much faster to zero than the pure homogeneous simulation. Heterogeneous recombination is therefore identified as an important loss reaction for HO₂ radicals in our cell.

From the above, we conclude that gas phase photolysis is a negligible process with the H₂O₂ concentrations typically used in our photocatalytic experiments, and that observed HO₂ radicals in the gas phase are due to the photocatalytic degradation of H₂O₂.

3.4. Influence of pressure and distance on the HO₂ concentration

In Fig. 6 HO₂ formation at 2 different pressures are presented: 33 and 233 Torr. Flow conditions were comparable in both cases ($100 \text{ STP cm}^3 \text{ min}^{-1}$), and absolute H₂O₂ concentrations have been measured by cw-CRDS absorption: assuming that the broadening coefficients for HO₂ radicals [24] are also valid for H₂O₂, we obtain H₂O₂ concentrations of 3.3 and $11 \times 10^{14} \text{ cm}^{-3}$ at 33 and 233 Torr, respectively. For both pressures, we observe again a steep, nearly instantaneous formation of HO₂, i.e. the same phenomenon as observed in the gas phase photolysis. While at 33 Torr the concentration immediately reaches the steady-state condition, at 233 Torr the HO₂ concentration decays for around 150 s before reaching a stationary condition. This behaviour is probably due to a depletion

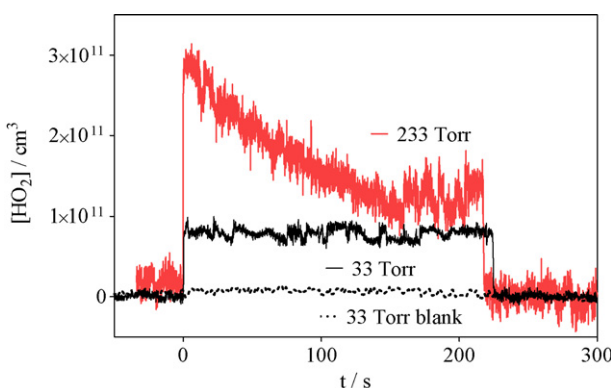


Fig. 6. HO₂ concentration time profiles for 2 different pressures: 233 Torr (upper, red curve) and 33 Torr (lower, black curve) together with blank experiment (dotted line). All experiments: $1 \text{ STP cm}^3 \text{ min}^{-1}$ O₂ bubbling through H₂O₂, $80 \text{ STP cm}^3 \text{ min}^{-1}$ synthetic air, 4 mm distance between surface and detection volume.

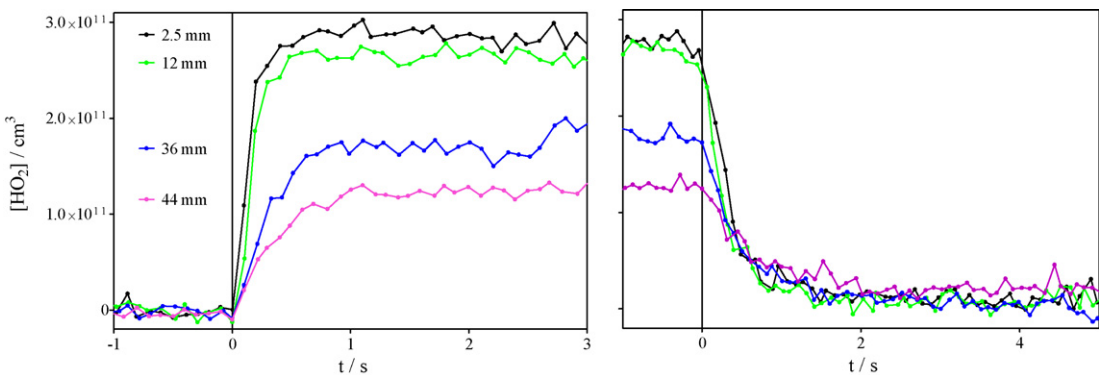


Fig. 8. HO₂ concentration time profile after turning on (left figure at $t = 0$ s) and off (right figure at $t = 0$ s) the UV-lamp; only small portions of signal similar to Fig. 6 are shown in zoomed form. Four different distances between the surfaces and the cw-CRDS beam. $p = 35$ Torr, $1 \text{ STP cm}^3 \text{ min}^{-1}$ O₂ bubbling through H₂O₂, $40 \text{ STP cm}^3 \text{ min}^{-1}$ synthetic air.

of H₂O₂ at higher pressure: the residence time is rather long (7 min compared to 1 min at 33 Torr) and HO₂ formation becomes limited by the supply of fresh H₂O₂.

Finally, we have tested the impact of the distance between the surface and the cw-CRDS beam: in Fig. 8 the results for four different distances between surface and detection beam are shown. Again, HO₂ concentrations become rapidly stationary and do not evolve over several minutes. Therefore, in this figure only the lamp-on and lamp-off parts of the signals are shown in a zoomed form for better visibility. HO₂ radicals are still observed in high concentrations even 44 mm above the surface. The time-evolution during the on- and off phase become slower with increasing distance between surface and detection volume: at 44 mm it takes 1 s to reach stationary conditions when turning on the UV-light and up to 2 s when turning off. We believe that this is due to a decrease in heterogeneous loss of the radicals on the photocatalytic surface.

4. Discussion

From the experiments presented in this paper it can be concluded without doubt that the photocatalytic degradation of H₂O₂ leads to the formation of free HO₂ radicals in the vicinity of the photocatalytic surface. However, the mechanism of its formation cannot clearly be elucidated from our experiments. Several possibilities might be considered:

- It is currently admitted that HO₂ is formed at the surface from a recombination between O₂, H⁺ and e⁻:



These radicals can be further reduced to H₂O₂ or might also recombine at the surface with other radicals like HO₂ or OH, however it is also possible that they subsequently desorb from the surface and diffuse into the gas phase.

- Another possible reaction path is the participation of OH radicals, also formed at the surface:



These OH radicals might then react with adsorbed H₂O₂ molecules on the surface generating HO₂ radicals which subsequently are released into the gas phase. However, OH radicals might as well desorb from the surface and form HO₂ radicals by reaction with H₂O₂ molecules present in the gas phase.

- Also one could imagine that desorbed O₂(¹Δ), formed in quantum yields of up to 0.38 [7], react in the gas phase with H₂O₂ molecules: however, from thermodynamic consideration this pathway can be ruled out, as it is an endothermic reaction ($\Delta H_f = +47.2 \text{ kJ mol}^{-1}$) [28].

Unfortunately, from the current experiments we cannot distinguish between these different possibilities, more detailed investigations will be necessary. Studying the evolution of the HO₂ radical concentration after addition of VOC vapour to the H₂O₂ mixture, as has been investigated using classical methods by Vorontsov [29], will possibly help to understand the mechanism. The presented technique of cw-CRDS allows the selective detection of isotopes, so the addition of well defined concentrations of deuterated VOCs such as CD₃OD can compete with H₂O₂ for OH radicals and would lead at least at short reaction times to the formation of HDO, CD₂O and DO₂, all species being selectively detectable in a time resolved manner by cw-CRDS. This way it should be possible to better elucidate the origin of the observed HO₂ radicals: a reaction of OH radicals, originating from H₂O and h⁺, with H₂O₂ (and CH₃OD) would lead at least partially to the above mentioned deuterated reaction products, while the pathway (R3) should only lead to HO₂. The use of isotopically labelled O₂ would give a very clear answer about the origin of HO₂: desorbed HO₂ from (R3) should be completely labelled, while HO₂ formed during the degradation of H₂O₂ should be unlabeled; however, financial considerations might prevent the conduction of such experiments.

5. Conclusion

We have presented for the first time the formation of HO₂ radicals in the vicinity of photocatalytic surfaces. This is also the first, direct detection of free radicals in the vicinity of photocatalytic surfaces using photon fluxes typical for photocatalytic experiments. The detection has been done by the selective and sensitive method of cw-Cavity Ring Down Spectroscopy. HO₂ radicals are clearly observed in the gas phase even at distances as far as 44 mm from the surface and at pressures of up to 230 Torr. A decrease of H₂O₂ concentration has also been observed by the same technique, leading to a lower limit of the quantum yield of 0.0024 for photocatalytic H₂O₂ destruction.

Acknowledgements

This work is jointly supported by the Nord-Pas de Calais region in the framework of the IRENI research program, by the French Research Ministry and by the European Fund for Regional Economic Development (FEDER). The authors thank F. Thevenet for the preparation of the photocatalytic support. A. Parker thanks the EU for financial support through project MEST-CT-2005-020659. C. Bahrini thanks the University Lille 1 for financial support.

References

- [1] A. Fujishima, K. Honda, *Nature* 238 (1972) 37–38.
- [2] A. Fujishima, T.N. Rao, D.A. Tryk, *J. Photochem. Photobiol. C: Photochem. Rev.* 1 (2000) 1–21.
- [3] J. Thiebaud, A. Parker, C. Fittschen, G. Vincent, O. Zahraa, P.-M. Marquaire, *J. Phys. Chem. C* 112 (2008) 2239–2243.
- [4] J.M. Langridge, R.J. Gustafsson, P.T. Griffiths, R.A. Cox, R.M. Lambert, R.L. Jones, *Atmos. Environ.* 43 (2009) 5128–5131.
- [5] J. Peral, D.F. Ollis, *J. Mol. Catal. A: Chem.* 115 (1997) 347–354.
- [6] A. Mills, S.L. Hunte, *J. Photochem. Photobiol. A: Chem.* 108 (1997) 1–35.
- [7] T. Daimon, Y. Nosaka, *J. Phys. Chem. C* 111 (2007) 4420–4424.
- [8] T. Tachikawa, T. Majima, *Langmuir* 25 (2009) 7791–7802.
- [9] T. Daimon, T. Hirakawa, M. Kitazawa, J. Suetake, Y. Nosaka, *Appl. Catal. A: Gen.* 340 (2008) 169–175.
- [10] Y. Shiraishi, T. Hirai, *J. Photochem. Photobiol. C: Photochem. Rev.* 9 (2008) 157–170.
- [11] M.C. Lee, W. Choi, *J. Phys. Chem. B* 106 (2002) 11818–11822.
- [12] J.S. Park, W. Choi, *Langmuir* 20 (2004) 11523–11527.
- [13] J.S. Park, W. Choi, *Chem. Lett.* 34 (2005) 1630–1631.
- [14] T. Tatsuma, S.I. Tachibana, A. Fujishima, *J. Phys. Chem. B* 105 (2001) 6987–6992.
- [15] T. Tatsuma, S.I. Tachibana, T. Miwa, D.A. Tryk, A. Fujishima, *J. Phys. Chem. B* 103 (1999) 8033–8035.
- [16] W. Kubo, T. Tatsuma, *Anal. Sci.* 20 (2004) 591–593.
- [17] W. Kubo, T. Tatsuma, *J. Am. Chem. Soc.* 128 (2006) 16034–16035.
- [18] Y. Murakami, E. Kenji, A.Y. Nosaka, Y. Nosaka, *J. Phys. Chem. B* 110 (2006) 16808–16811.
- [19] Y. Murakami, K. Endo, I. Ohta, A.Y. Nosaka, Y. Nosaka, *J. Phys. Chem. C* 111 (2007) 11339–11346.
- [20] G. Vincent, A. Aluculesei, A. Parker, C. Fittschen, O. Zahraa, P.-M. Marquaire, *J. Phys. Chem. C* 112 (2008) 9115–9119.
- [21] J. Thiebaud, F. Thevenet, C. Fittschen, *J. Phys. Chem. C* 114 (2010) 3082–3088.
- [22] J. Thiebaud, C. Fittschen, *Appl. Phys. B: Lasers Opt.* 85 (2006) 383–389.
- [23] J. Thiebaud, S. Crunaire, C. Fittschen, *J. Phys. Chem. A* 111 (2007) 6959–6966.
- [24] N. Ibrahim, J. Thiebaud, J. Orphal, C. Fittschen, *J. Mol. Spectrosc.* 242 (2007) 64–69.
- [25] A. Parker, C. Jain, C. Schoemaecker, P. Sriftgiser, O. Votava, C. Fittschen, PCCP, submitted for publication.
- [26] J. Thiebaud, A. Aluculesei, C. Fittschen, *J. Chem. Phys.* 126 (2007) 186101.
- [27] R. Atkinson, D.L. Baulch, R.A. Cox, J.N. Crowley, R.F. Hampson, R.G. Hynes, M.E. Jenkin, M.J. Rossi, J. Troe, *Atmos. Chem. Phys.* 4 (2004) 1461–1738.
- [28] NIST Chemistry webbook: <http://webbook.nist.gov/chemistry/>.
- [29] A.V. Vorontsov, *Catal. Commun.* 8 (2007) 2100–2104.